Research

Ecography 34: 488–497, 2011
doi: 10.1111/j.1600-0587.2010.06326.x
© 2011 The Authors. Ecography © 2011 Ecography
Subject Editor: Jacques Régnière. Accepted 12 August 2010

Pattern analysis of eastern spruce budworm *Choristoneura fumiferana* dispersal

Dean P. Anderson and Brian R. Sturtevant

D. P. Anderson, Landcare Research, PO Box 40, Lincoln, New Zealand. – B. R. Sturtevant, Inst. for Applied Ecosystems Studies, U.S. Forest Service, Northern Research Station, 5985 Hwy K, Rhinelander, WI 54501, USA.

Dispersal has been proposed as an important mechanism in the broad-scale synchronisation of insect outbreaks by linking spatially disjunct populations. Evidence suggests that dispersal is influenced by landscape structure, phenology, temperature, and air currents; however, the details remain unclear due to the difficulty of quantifying dispersal. In this study, we used data on the abundance and distribution of spruce budworm *Choristoneura fumiferana* larvae (potential dispersers) and adult male moths (dispersers) to make inference on the effects of air currents and host-species abundance on dispersal. Hierarchical-Bayesian and inverse modeling was used to explore 4 dispersal models: 1) isotropic dispersal; 2) directional-dispersal; 3) directional-and-host-species dispersal; and 4) host-species dispersal. Despite their strong dependence on balsam fir *Abies balsamea* and spruce species *Picea* spp., the mapped basal area of these host species did not influence the pattern of dispersed moths. The model that best fit the data was the directional-dispersal model, which showed that the prevailing dispersal direction was from the northwest (328°). We infer that the strong pattern of directional dispersal was due to a prevailing wind from the same direction. Our interpretation was corroborated by independent wind data during the period of active adult male budworm flight, particularly in the region with high larval abundance. Our results indicate that there was a relatively high probability of individuals flying at least 48 km with the wind where larvae abundance at source locations was also high. Such findings emphasize the importance of long-distance dispersal on spatial distribution of adult male spruce budworms. Insight into the population-level consequences of such dispersal patterns requires additional research.

Insects and disease impact the largest area of U.S. forests relative to other disturbance types, affecting an estimated 50 million acres with economic costs over $1.5 billion (Dale et al. 2001). Economic impacts are exacerbated by the regional synchronization of insect outbreaks, which increases damage intensity (Candau et al. 1998, Cooke and Lorenzetti 2006, Johnson et al. 2006) and overwhelms agency and industry mitigation resources. Insect dispersal can link independently oscillating populations, synchronizing the dynamics of spatially disjunct populations (Kaitala and Ranta 1998, Williams and Liebhold 2000, Peltonen et al. 2002, Tobin and Bjornstad 2005). While evidence supports the idea that regional synchrony and other spatiotemporal outbreak patterns may be caused by dispersal of insects from areas of high to low abundance (Royama 1984, Williams and Liebhold 2000, Johnson et al. 2004, Nealis and Régnière 2004a, Royama et al. 2005), the role of dispersal in explaining these patterns remains unclear due to the difficulty of quantifying dispersal and its impacts on populations (Royama 1984, Royama et al. 2005). A greater understanding of the processes underlying dispersal may improve our ability to predict outbreak spread and focus effective intervention measures (Greenbank et al. 1980, Sharov and Liebhold 1998, Johnson et al. 2006).

Increasing evidence suggests that dispersal varies spatially and temporally as a function of landscape structure (Keyghobadi et al. 1999, 2006, Cooke and Roland 2000, Nathan et al. 2005), vegetation phenology (Gage et al. 1999), temperature (Sanders et al. 1978), and the direction and speed of air currents (Greenbank et al. 1980, Onstad et al. 2003). Several forest and agricultural pests have been shown to use wind either actively or passively to enhance their dispersal (Greenbank et al. 1980, Riley et al. 1991, Westbrook and Isard 1999, Onstad et al. 2003). In combination with air currents, it is likely that host-species distribution may influence how dispersing forest-insect pests move and settle (Roland 1993, Bergeron et al. 1995, Su et al. 1996, Cooke and Roland 2000).

The objective of this study was to use data on the abundance and distribution of spruce budworm (SBW) *Choristoneura fumiferana* larvae (potential dispersers) and adult male moths (dispersers) to make inference on the effects of air currents and host-species abundance on dispersal. We used a hierarchical Bayesian approach to estimate a dispersal kernel from source locations

(Clark et al. 1999, Walder et al. 2009) using four alternative dispersal models. First was an ''isotropic-dispersal model'' that results in movement away from the source without directional bias or the influence of host-species abundance. Second was a ''directional-dispersal model'', in which movement away from the source was biased in one direction (presumably due to wind) but not influenced by host-species abundance. Third was a ''directional-and-landscape-dispersal model'', in which movement had a directional bias and was influenced by host-species abundance. Lastly, we examined a ''landscape-dispersal model'', in which movement was only contingent on the abundance of host species. While we do not directly incorporate wind data into our analyses, we infer that directional dispersal would most likely be due to air currents.

Hierarchical Bayesian and inverse-modeling has been applied to isotropic and, to a lesser extent, anisotropic (directional) models of seed dispersal (Clark 1998, Clark et al. 1999, Stoyan and Wagner 2001, Wagner et al. 2004, Martinez and Gonzalez-Taboada 2009, Walder et al. 2009), but has not previously been applied to insect dispersal. While trees are distinct point sources of dispersing seeds and fruits, it was not possible to empirically measure the larvae abundance (point sources of dispersers) across the continuous surface of our study area. Consequently, a key element of our Bayesian hierarchical model was to generate larvae abundance data by kriging data from larvae-collection locations to obtain a continuous surface of larval abundance, which represented the distribution of potential dispersers. We then used the spatial pattern of moths trapped at point locations to statistically estimate parameters for a dispersal kernel and landscape covariates (Clark 1998, Clark et al. 1999). We examined a Gaussian kernel whose shape could be modified by decay and directional-bias parameters, which allowed for anisotropic models (Wagner et al. 2004, Walder et al. 2009). Consequently, we were able to examine relatively simple field data and make important inferences on dispersal patterns of spruce budworm. Lastly, we analysed wind data during dispersal periods to compare with modelled directional dispersal patterns.

Methods

Study system

Spruce budworm is a native insect that periodically (~35 yr cycle) defoliates balsam fir *Abies balsamea* and spruce species *Picea* spp. in the boreal and sub-boreal forests of North America. Females lay eggs on fir and spruce species but do not appear to differentiate among different host species (Nealis and Régnière 2004b). Eggs hatch in 10 d, and the first-instar larvae disperse a short distance within the tree or stand. The larvae form hibernacula, in which they molt into second-instar larvae and enter into winter diapause. The larvae emerge in early May and begin feeding on host tree foliage. Pupation occurs in mid-June, and moths eclose in approximately 10 d, completing the cycle. Local phenology of SBW life stages is strongly related to temperature (Régnière and You 1991). Moth dispersal occurs in the evenings and is dependent on meteorological conditions (Greenbank et al. 1980). While there may be subtle differences in the timing of exodus between male and female moths, both sexes emigrate together and have identical exodus characteristics (Greenbank et al. 1980). Females may emigrate after laying part of their egg complement at the place of emergence. Moths can easily disperse 20 km and the maximum recorded dispersal distance is 450 km (Greenbank et al. 1980). In addition, evidence indicates that emigration rates increase with increasing levels of defoliation (Royama 1984, Nealis and Régnière 2004a).

The study area covers ca 69 000 km^2 and is centered on the border lakes ecoregion between Ontario, Canada and Minnesota, USA, hereafter referred to as Border Lakes Landscape (BLL, Fig. 1). The central portion is a large (1 million ha) unmanaged wilderness area comprised of the Boundary Waters Canoe Area Wilderness, Voyageurs

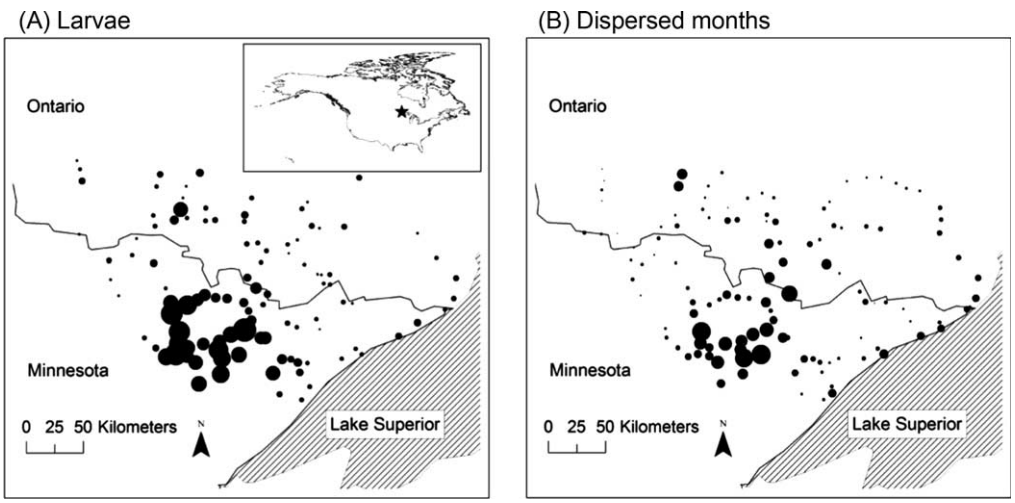

Figure 1. Maps of Border-Lakes Landscape study area along the Minnesota–Ontario border, indicating the collection locations and relative abundances of larvae (A) and moths (B). The black circles represent the varying values of relative-larval abundance (0–2.5 larvae per person-min) and moth counts (1–453).

National Park, and the Quetico Provincial Park. Surrounding the wilderness areas are highly managed landscapes in the US and Canada.

Larvae collection

We collected SBW larvae at 147 sites (Fig. 1A) over a two-week period in June 2007. This period coincided primarily with the largest (4th–6th instar) larvae stages. Site selection was based on the presence of multiple trees of balsam fir and white spruce. Larvae were collected by hand up to 2.3 m above ground or with pole pruners up to 4.5 m above ground. Specimens were preserved in ethanol and confirmed to species level in the laboratory. We recorded the search time at each site. We generally searched until 20 larvae were obtained or until approximately 60 person-min had elapsed. In our analyses, we used the number of larvae collected divided by the person-minutes as a relative measure of larvae abundance at each site.

Moth collection

At 120 of the larvae collection sites we placed 3 traps baited with polyethylene caps containing eastern SBW pheromone (E-11-Tetradecenal; Z-11-Tetradecenal; Scentry Biologicals) and containing insecticidal vaportape (Dimethyl-2, 2-dichlorovinyl phosphate; Hercon Environmental) for capturing male moths (Fig. 1B). We used a of combination universal traps (UniTrap) and Multipher 1 traps (approximately equal numbers of each) that have similar moth capture rates (Mullen et al. 1998). Hereafter, we use "moths" to represent adult male moths. The moth collection sites were generally no closer than 8 km in proximity, but in a few cases they were separated by only 6 km. Traps were hung from branches of balsam fir or white spruce ca 5–10 m apart prior to the flight period. Moths were removed from traps outside the wilderness area every 7–10 d during the main flight period (late June through mid-July) and a final collection at the end of August. Within wilderness areas without road access, samples were collected once during a two-week period from early to mid-August. Final collection at all sites was after the end of the flight period. In the laboratory, all SBW individuals were identified and tallied under a 20 × dissection microscope.

Landscape covariates

In our analyses we considered landscape covariates related to forest structure and defoliation by SBW. We obtained GIS data at 30-m resolution on the basal area for balsam fir *Abies balsamea,* spruce species *Picea* spp., and deciduous species (Wolter et al. 2009). Commission errors with non-host conifers (e.g. *Pinus* spp.) were corrected by constructing a non-host conifer mask, defined as locations where nonhost conifers were present and host-species basal area was <15% of the total basal area (P. T. Wolter, Univ. of Wisconsin-Madison, pers. comm.). ArcMap (ESRI 2006) was used to calculate the total basal area of these species within a 500-m radius around moth collection sites. A GIS map depicting areas defoliated by SBW based on aerial surveys conducted in 2007 was obtained from the U.S. Forest Service (<http://na.fs.fed.us/fhp/ta/av/index.shtm>; accessed March 2008).

Data modeling

We used Bayesian hierarchical modeling on spatially referenced larvae- and moth-abundance data to make inference on moth dispersal patterns in the BLL (Fig. 2). Moth counts at each site were potentially influenced by landscape covariates at that site, as well as the dispersal pattern of moths (redistribution kernel). The redistribution kernel could be influenced by decay and directional parameters, and the relative number of potential dispersers (relative-larval abundance). Inference was made by factoring the high dimensional hierarchical model into lower dimensional

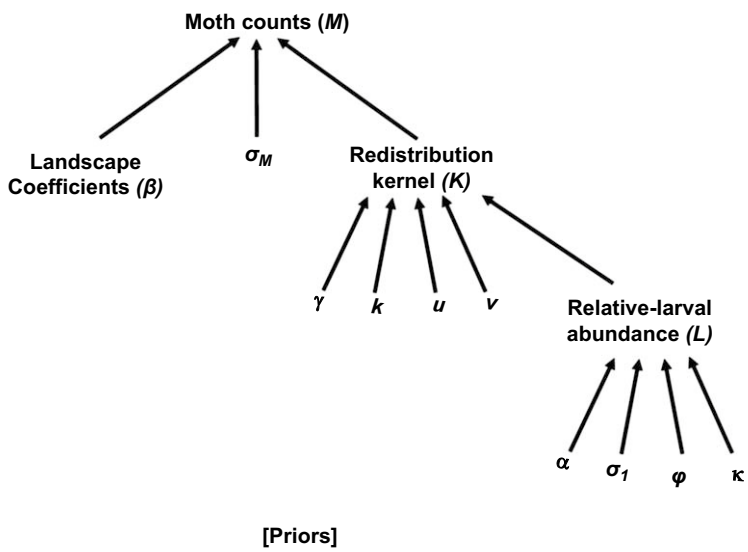

Figure 2. Directed graph of parameter dependencies used in the Bayesian hierarchical model.

conditional probabilities that were easy to compute (Wikle 2003).

Relative-larval-abundance sub-model

The purpose of the relative-larval-abundance sub-model was to krige larvae-collection data to create a continuous surface of relative-larvae abundance across the study area. Fourth to sixth instar larvae were considered potential dispersers; therefore the relative-larval-abundance sub-model occupies the lowest portion of the model hierarchy, aside from priors on parameters (Fig. 2). We used Bayesian kriging (Clark 2007, pp. 408–410) to extrapolate the observed relative-larval abundance to points on a 8-km grid system, hereafter referred to as grid-point prediction sites. The relative-larval abundance observed (L_g) at site g follows a multivariate normal distribution:

$$\ln(L_g) = \alpha X_g + \varepsilon_L$$

$$\varepsilon_L \sim N(0,\ C_{g,g'})$$

$$C_{g,g'} = \sigma_L^2 \exp(-(\varphi d_{g,g'})^s)$$

where αX_g was the matrix product of coefficients and covariates, and $C_{g,g'}$ was the spatial covariance matrix described by a variance (σ_L) and a distance correlation parameter (φ), and the distance among larvae collection sites ($d_{g,g'}$). We added 0.004 to L_g and performed a natural log transformation to normalise the data. In this model the only coefficients were for the intercept and a covariate derived from aerial survey data on defoliation (see below).

Our GIS data on forest structure did not extend outside the study area (Fig. 1), which created edge-effect problems in our analysis. Consequently, the only covariate used in the kriging was distance-weighted defoliation *($defol_g$)* of SBW at larvae collection sites g. This covariate represents a relative measure of proximity to all defoliated areas from larvae collection points. The distance-weighted defoliation was calculated by first placing random points h within the defoliation polygons at a rate of 2.5 points km^{-2}. We then calculated the distance between each larvae collection site and each generated random point across all defoliation polygons ($d_{g,h}$). Similarly, we calculated the distance between grid-point prediction sites i and each generated random point ($d_{h,i}$). *The* $defol_g$ variable was calculated as follows:

$$defol_g = \sum\nolimits_{g,h} \exp(-d_{g,h}).$$

Similarly, the distance weighted defoliation at grid-point prediction sites $defol_i$ was:

$$defol_i = \sum\nolimits_{h,i} \exp(-d_{h,i}).$$

The predicted relative larval-abundance (L_i) at 8-km grid points i followed a multivariate normal distribution (Clark 2007):

$$E(\ln(L_i)\,|\,L_g, \alpha, \sigma_L, \varphi, s) = \alpha X_i + C_{g,i}^T C_{g,g'}^{-1}(\ln(L_g) - \alpha X_g)$$

$$\mathrm{var}(\ln(L_i)\,|\,L_g, \alpha, \sigma_L, \varphi, s) = C_{i,i'} - C_{g,i}^T C_{g,g'}^{-1} C_{g,i}$$

$$C_{g,i'} = \sigma_L^2 \exp(-(\varphi d_{g,i'})^s)$$

$$C_{i,i'} = \sigma_L^2 \exp(-(\varphi d_{i,i'})^s)$$

where $C_{g,i}$ was the spatial covariance matrix among larvae collection points (g) and prediction grid points (i), $C_{i,i}$ was the covariance matrix among prediction grid points, and s was a smoothing parameter.

We used Markov chain Monte Carlo (MCMC) to fit the kriging-model parameters. The regression coefficients (α) were sampled directly from the conditional posteriors using vague priors (Normal(α|0,1000)). The spatial covariance parameters (σ_L, φ) were sampled with a Metropolis-Hastings rejection algorithm, using lognormal priors: Normal($\ln(\sigma_L)$|ln(3),1) and Normal($\ln(\varphi)$|ln(1),1). Parameter estimates and the associated uncertainty in estimates of the relative-larval abundance were propagated into the moth-dispersal sub-model.

Moth-dispersal sub-model

The predicted relative-larval abundance at the 8-km grid points was used to derive a dispersal kernel that in turn was used as a parameter of moth-dispersal model. We explored various models that explained the number of moths captured (M_j) at moth collection sites j as a function of a dispersal kernel and landscape covariates (X_j), such as basal area of fir, spruce and deciduous trees:

$$\ln(M_j) = \beta X_j + \ln(K_j) + \varepsilon_j$$

$$\varepsilon_j \sim N(0, \sigma_M^2)$$

where the variable K_j was the estimated dispersal kernel value (or, a relative measure) of moths arriving from all grid point locations within 48 km of the moth-collection site, and β represents the coefficients for the landscape covariates. The X_j were natural-log transformed to increase efficiency of MCMC convergence on model parameters. The errors were assumed to be independent and identically distributed with variance σ_M^2. The dispersal kernel had the following form:

$$K_j = \sum\nolimits_{i,j} e^{-Dist_{i,j}^2/2L_i\gamma^2},$$

where γ was a decay parameter, $Dist_{i,j}$, was the "effective distance" between the source of moths at prediction-grid point i and the moth collection site j. The variable $Dist_{i,j}$ was the Euclidian distance adjusted by parameters that describe directionality, amplitude (or strength), and the focus of directional dispersal. The variable $Dist_{i,j}$ was obtained by the product of the Euclidian distance ($d_{i,j}$) and a directional function, which is a generalisation of the von Mises distribution (Batschelet 1981, Wagner et al. 2004):

$$Dist_{ij} = d_{i,j} \times \exp(k \cdot \cos(\delta_{ij} - u + v \times \sin(\delta_{ij} - u)))$$

where δ is the angle in radians between larvae source (i) and the moth trap (j), parameter k determines the amplitude, u is the phase parameter (direction ranging from $-\pi$ to π and 0 is north), and parameter v determines the directional focus of the directional dispersal kernel. We found that the decay (γ) and the amplitude (k) parameters were highly correlated, which prevented convergence when attempting to fit a directional dispersal kernel model. Both of these parameters govern how far moths are likely to fly from the source location. Consequently, when fitting a directional kernel, we set γ equal to 1, and let the decay be dictated by

the k parameter. When fitting an isotropic kernel, the directional parameters were not included and γ was not constrained to 1. The isotropic kernel depended on the Euclidian distance and L_i:

$$K_j = \sum_{i,j} e^{-d_{i,j}^2/2L_i\gamma^2},$$

We were constrained by the distance at which we could allow larvae abundance to influence moth counts because we did not have larvae abundance estimates in a large area around the study area. For this reason we allowed moth dispersal to influence moth counts at a maximum distance of 48 km. Consequently, while we had 120 moth-collection sites, we modelled moth counts at the 67 sites located in the core of the study area.

In the moth-dispersal model, the regression coefficients (β) and variance (σ_M^2) were sampled directly from the conditional posteriors using prior distributions Normal (β | 0,1000) and InverseGamma (σ_M^2| 2,2) respectively. The natural-log transformation normalised the moth count data ($M\hat{j}$), which allowed us to efficiently sample the conditional posteriors, as opposed to modelling these data as a Poisson process, which has been done in seed-dispersal studies (Clark et al. 1999, Stoyan and Wagner 2001, Martinez and Gonzalez-Taboada 2009). In isotropic kernel models, γ was sampled with a Metropolis-Hastings rejection algorithm, using lognormal priors: Normal ($\ln(\gamma)$ | $\ln(1)$,1). For anisotropic kernels, the directional parameters were sampled with a Metropolis-Hastings rejection algorithm with the following prior distributions: Normal (k| 0,10); Uniform(u | $-\pi$,π); and Uniform(v | -1,2). Within-chain serial autocorrelation was assessed to determine the appropriate thinning rate. Convergence on the posterior target distribution was confirmed with a scale reduction factor ($\hat{R}$) <1.2 calculated on 4 parallel chains (Gelman and Rubin 1992, Gelman et al. 2004). Convergence was achieved with 200 000 iterations, and posterior summaries were taken from 4 chains containing 100 000 samples with a thinning rate of 10 (i.e. 40 000 samples). We used the Deviance Information Criterion (DIC; Spiegelhalter et al. 2002) and R^2 to compare competing models.

Evaluation of prevailing winds

Prevailing wind directions during periods of active adult male budworm flight across the study area were quantified as an independent validation of our modelling results. Archived hourly wind and temperature observations from the summer of 2007 were downloaded from both Canadian and U.S. weather station sources distributed across the study area. U.S. observations were obtained from the Remote Automated Weather Station (RAWS) network (16 stations; <www.fs.fed.us/raws/standards.shtml>). Canadian observations were obtained from the Environment Canada National Climate Data and Information Archive (4 stations; <http://climate.weatheroffice.gc.ca>). We added 180° to each reported wind direction to transform the data from source direction (i.e. where the wind came from) to the direction of wind travel.

Both wind fields and SBW phenology (defining the adult male flight period) were expected to vary significantly across the study area. We therefore defined "prevailing winds" as the wind direction and velocity associated with each larvae-sampling point during the estimated active flight period for each respective point. We assigned each larvae-sampling point to their nearest weather station. We then extracted only those observations that met the following biological criteria: 1) minimum flight temperature of 15°C; 2) minimum wind velocity of 0.7 ms^{-1}; 3) time of active flight (19:00–24:00 h local daylight time); and 4) dates of active flight based on SBW phenology for a given sampling point. Criteria 1–3 were derived from Greenbank et al. (1980). Criteria 4 was estimated using the SBW phenology model (Régnière 1982) as implemented in BioSIM (v9.5.1; Régnière and Saint-Amant 2004). BioSIM simulates emergence and life stages of SBW and other forest insect pests using NOAA/NCDC weather station data interpolated over a digital elevation model. The timing of adult SBW emergence is influenced by temperature and precipitation. We output three dates for each insect sample point corresponding with 10% adult male emergence, peak adult male emergence, and 90% adult male emergence. Active flight dates for a given sample point was defined as the range of dates between 10% adult male emergence and 90% male emergence for that point. This range always contained the peak emergence date, and contained on average a 20-d period.

Hourly observations meeting the above flight criteria were grouped into 8 compass directions (north, northeast, east . . .). Directionality in wind data were quantified in two ways: frequency of observations and the potential passive transport distance for the active flight period. The latter was estimated by summing the wind velocities (km h^{-1}) within each cardinal direction for a given sample point, interpreted as the distance (km) a particle would travel in a given direction from the sample point if airborne for the entire active flight period (dates and hours). Prevailing wind variables were averaged across all sample points (n = 137), and also across a subset of sample points with larvae abundances >0.75 larvae min^{-1} of searcher effort (n = 19). This threshold in larvae abundance corresponded well with the area of active defoliation in the southwestern part of the study area.

Results

Relative-larval-abundance sub-model

Across all sites where larvae abundance was measured, the lower-quartile, median, upper-quartile and maximum values for the relative-larval abundance were 0.02, 0.07, 0.23 and 2.5 respectively. Results of the kriging model of relative-larval abundance indicate an important effect of the distance-weighted defoliation variable (Table 1). The posterior distribution was positive and the 95% credible interval did not overlap zero, therefore this variable was retained. This result indicates, as expected, that defoliation increased with increasing relative-larval abundance. We used the posterior distributions of the covariance parameters to plot a theoretical variogram including the 95% credible intervals (Fig. 3). The variogram suggests that the spatial dependence in relative-larval abundance not

Table 1. Results of kriging model of relative-larval abundance. Summary statistics are from posterior distributions.

Parameters	Coefficient mean	Coefficient SD	Lower 95% CI	Upper 95% CI
Intercept	−2.33	0.67	−3.74	−1.03
Distance-weighted defoliation (*defol*)	0.24	0.07	0.11	0.38
Correlation (*p*)	0.77	0.48	0.15	2.00
Smoothing (*s*)	0.40	0.08	0.23	0.57
Variance	2.87	0.53	2.06	4.13

accounted for by the distance-weighted defoliation covariate extends out to a distance of 50 km (the distance at which the curve begins to level off).

Moth-dispersal sub-model

We explored 4 models of moth count data: isotropic dispersal; directional dispersal only; directional dispersal and landscape effects; and landscape effects only. The isotropic model fit the data reasonably well with an R^2 of 0.28 (Table 2). Our analysis clearly shows that the directional-dispersal-only model was the best as indicated by R^2 and DIC values. The 95% credible intervals for all landscape effects (individual basal areas of host and deciduous species) overlapped with zero in both models containing landscape variables, indicating a negligible effect on moth counts. There was substantial variation in the basal area of host species among sites, which should have resulted in significant landscape effect if SBW were responding to host species at the measured scale. For balsam fir, for example, the minimum, median and maximum basal area values within the 500-m radius buffer were 0.46, 31.93 and 127.00 m^2 ha^{-1} respectively. In the directional-dispersal-only model, the mean of the posterior distribution of the *k* (amplitude) parameter was 1.70, which indicates a strong directional effect (Table 3). The mean posterior value for the *u* (directional) parameter was −0.55, which shows that the prevailing dispersal direction was from the northwest (328°) to the southeast (148°). We infer from this result that this was the prevailing wind direction during the flight period.

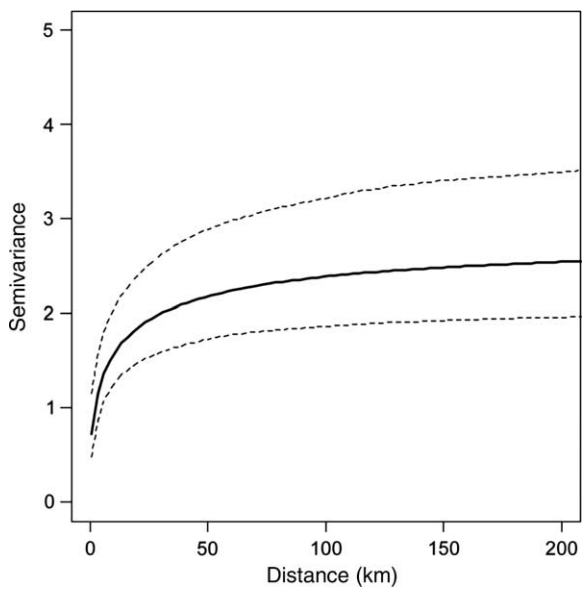

Figure 3. Theoretical semivariogram generated with covariance parameters showing the spatial dependence of the relative-larval abundance not accounted for by the distance-weighted defoliation covariate. Dashed lines are the 95% credible intervals.

Because of edge effects, we were only able to predict the shape of the dispersal kernel up to 48 km from a particular source location. The probability of a specific site receiving moths flying with the prevailing wind from 48 km away varied greatly as a function of the relative-larval abundance at the source location (Fig. 4). The model predicts that there was a probability of 0.65 that a source location with a relative-larval abundance value of 1 would contribute moths to a site 48 km downwind. With a relative-larval abundance value of 0.01, very few moths would fly >10 km with the prevailing wind. Because of the strong directional effect, the probability of sites receiving moths flying against or perpendicular to the wind was greatly reduced (Fig. 5).

Prevailing winds

We found anisotropy in wind direction when summarized across all insect sample points during their respective periods of active SBW flight, indicating positive bias in wind direction of travel ranging between north and southeast (Fig. 6A). Wind frequencies were highly correlated with the potential distance of travel ($\rho = 0.99$; only potential distances are shown). Restricting the sample points to those with high larvae abundance indicated a much stronger directional bias toward the southeast (Fig. 6B). Greater average potential distances in Fig. 6B also indicate stronger wind velocities in the vicinity of the insect sample points with high larvae abundance.

Discussion

Despite the crucial role of dispersal in metapopulation models (Pulliam 1988, Kareiva 1990, Hanski et al. 1995), it remains difficult to evaluate the relative importance of abiotic and biotic factors influencing emigration rates and long-distance dispersal because dispersal is difficult to measure. For Lepidopteran forest defoliators, dispersal has been indirectly inferred by examining egg to moth ratio, (Royama 1984, Nealis and Régnière 2004a, Royama et al. 2005), but this approach gives no information on how far

Table 2. Comparison of moth dispersal models using R^2 and DIC.

Model	R^2	DIC
Directional dispersal only	0.46	219.1
Directional dispersal+balsam fir basal area	0.44	220.7
Isotropic dispersal	0.28	238.5
Balsam fir basal area only	−0.06	267.9

Table 3. Summary statistics of the posterior parameter distributions for the directional-dispersal-only model.

Parameters	Mean coefficient	SD	Lower 95% CI	Upper 95% CI
Intercept	1.73	0.43	0.80	2.44
k (amplitude)	1.70	0.23	1.25	2.15
u (direction)	−0.55	0.31	−1.14	0.01
v (focus)	−0.09	0.54	−0.93	1.09
Variance	0.65	0.07	0.52	0.81

or where dispersers go. Mark–recapture studies provide information on spatial patterns of dispersal, but studies of long-distance dispersal (i.e. 10's of km) of insects using this technique are rare (Ockinger and Smith 2008). Microsatellite DNA analyses are being used increasingly to examine dispersal and gene flow (Pritchard et al. 2000, Blanchong et al. 2002, Lucchini et al. 2002, Manel et al. 2002), and to relate genetic structure to landscape features (Keyghobadi et al. 1999, Manel et al. 2003, Rueness et al. 2003, Wisely et al. 2004). The combination of hierarchical Bayesian and inverse-model fitting in the present study allowed us to use easily collected field data to make inference on patterns of SBW dispersal without actually identifying dispersing individuals. While inverse-model fitting has been widely employed in modelling seed dispersal (Clark 1998, Clark et al. 1999, Stoyan and Wagner 2001, Wagner et al. 2004, Martinez and Gonzalez-Taboada 2009, Walder et al. 2009), our study was, to our knowledge, the first attempt with insects. This empirical approach may therefore compliment more field or laboratory-intensive methods to investigate long-distance dispersal of mobile organisms.

The kriged grid of relative-larval abundance represented the distribution of potential dispersers, which were used with inverse modelling to identify the dispersal model that best explained the spatial distribution of dispersed adult moths. Our grid system had an 8-km resolution because this was the primary distance that separated our larvae and moth collection sites. For our kriging model, consequently, we needed to quantify any potential covariates at that resolution. This created edge-effect problems for quantifying the total basal area of host species, because our GIS data on host-species basal area did not extend outside of the study area. As a result, we were not able to accurately quantify the basal area of host species at the 8-km resolution. We did find, however, that the amount of SBW defoliation in the area (as measured by the distance-weighted defoliation variable) was an important explanatory variable of the relative-larval abundance. Model predictions may have been better if we had the appropriate GIS data (i.e. data outside the study area).

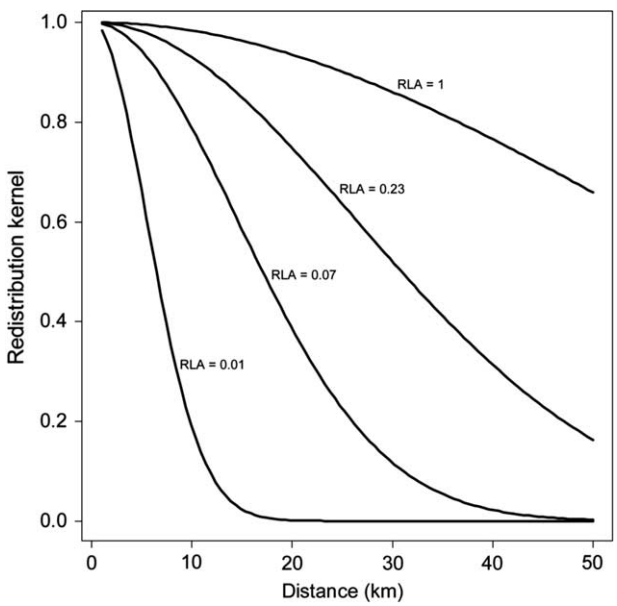

Figure 4. Redistribution kernel of moths flying with the prevailing wind from a single source location with relative-larval abundance (RLA) levels of 0.01, 0.07, 0.23 and 1. The kernel values represent a relative measure of moths arriving at the destination location.

Model comparison showed that dispersal patterns were best explained by a model that incorporates directional dispersal, presumably due to wind effects, but was not influenced by host-species abundance. Our modelling allows for a single directional effect over the entire study area and over the entire flight period. Examination of the available wind data indicated that wind directions varied both spatially and temporally, which presumably appeared as noise in our data as we made inference over the entire flight period. Consequently, the strong dispersal pattern was due either to a single or few days of strong winds in the stated direction or that the prevailing wind was consistently in that direction. The strong directional signal in the dispersal kernel indicates that the bulk of the moths flew from the northwest to the southeast. While our study was limited to one dispersal season, the strong directional pattern clearly suggests that across years SBW dispersal should be directional, but the direction and dispersal distances will vary according to wind conditions.

Independent analyses of weather station data from across the study area show evidence of a prevailing wind direction during periods of active SBW flight (Fig. 6). It is impossible to know the wind direction at the time of flight, but these results support our conclusion that wind currents enhance directional dispersal. Weather station data was most consistent with our dispersal model when restricted to the region with high larvae abundance, corresponding primarily with a localized area of defoliation in the southwestern part of the study area (Fig. 1A). The stronger corroboration between the wind analysis and modelling results in the high-density southwest area could be due to model results being dominated by locations with high numbers dispersers or by density-dependent dispersal behaviour. Nealis and Régnière (2004b) demonstrated that female adult SBW were most likely to emigrate in high density situations where food resources were depleted via defoliation. Our pheromone traps, however, only attract males, and it remains unknown whether such density-dependent responses affect the emigration behaviour of adult male SBW.

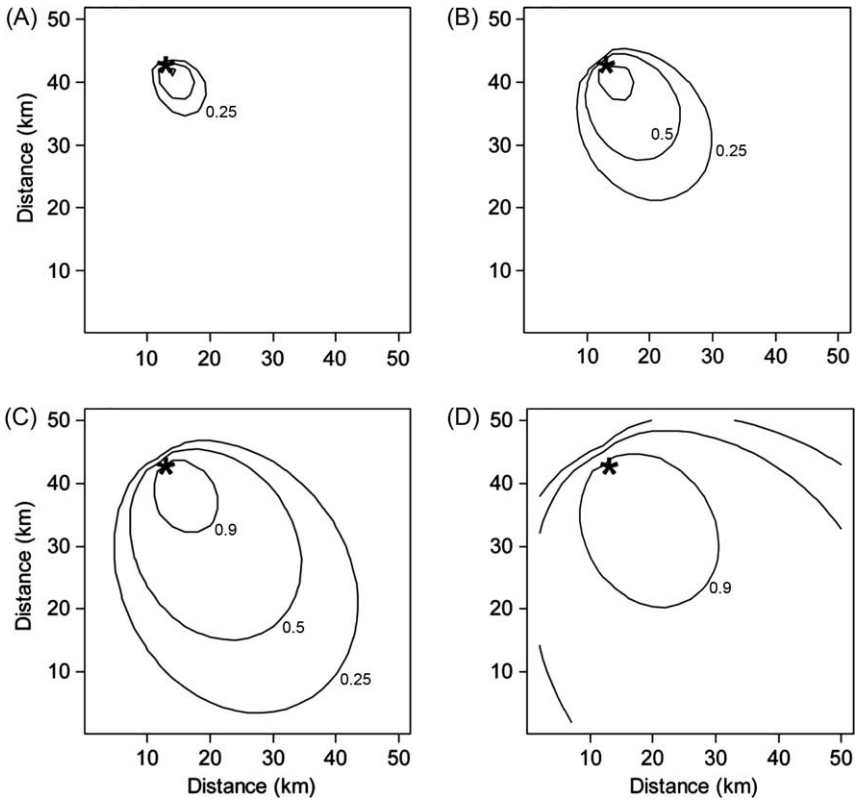

Figure 5. Two-dimensional redistribution kernel of moths flying from a single source location with relative-larval abundance levels of 0.01 (top left), 0.07 (top right), 0.23 (bottom left) and 1 (bottom right). The kernel values represent a relative measure of moths arriving at the destination location.

Our conclusion that SBW used air currents to facilitate dispersal is consistent with previous findings on dispersal by SBW and other vagile insect pests (Greenbank et al. 1980, Riley et al. 1991, Westbrook and Isard 1999, Onstad et al. 2003). Given the results that SBW flying with the wind can easily travel 48 km, and probably much further if we extrapolate beyond our data, it is very likely that dispersal is capable of synchronising independently oscillating populations (Kaitala and Ranta 1998, Williams and Liebhold 2000). An assumption underlying this conclusion is that our dispersal model is valid for both male and female moths. While females may disperse shorter distances than males, they also use air currents and disperse directionally (Green bank et al. 1980). A detailed population study demonstrated that net immigration of egg-bearing females affects local population dynamics (Nealis and Régnière 2004b). We, therefore, adhere to the results-supported conclusion that directional dispersal can facilitate synchrony.

Despite the strong dependence of SBW on balsam fir and spruce species, our analysis did not detect an important relationship between host-species basal area and moth-dispersal patterns. This is counter intuitive because evidence suggests that dispersing SBW deliberately descend onto host trees (Greenbank et al. 1980). Further, SBW population and defoliation dynamics are closely linked to the abundance and quality of host species (Bergeron et al. 1995, Su et al. 1996, Cappuccino et al. 1998, Cooke and Roland 2000, Zhang and Alfaro 2003). The lack of a relationship in our analysis may be a result of the fine-grained distribution of host species (small patches; James 2009) relative to broad-scale long-distance dispersal. All of our moth capture sites were situated in forest patches that contained one or both of the primary host species. It remains unknown how much host needs to be present to attract dispersing moths. A few isolated trees may be sufficient if they lie in the dispersing path. Our results show that the settling of dispersing moths is not related to broad-scale abundance of hosts (500-m buffer).

The approach presented here offers a flexible means to use data easily collected in the field and compare various forms of dispersal kernels in conjunction with landscape covariates (Clark et al. 1999). The results demonstrate compelling evidence for the directional redistribution of adult SBW via long-distance dispersal, at least when underlying populations are spatially heterogeneous as observed in this study. Future research should focus on the environmental and atmospheric processes underlying long-distance dispersal of adults, and quantify the effect of such movement on broad-scale population structure and, ultimately, outbreak synchrony.

Acknowledgements – This work was supported by the United States Dept of Agriculture, Cooperative State Research Education and Extension Service, National Research Initiative Grant no. WISR-2005-02815, and the National Fire Plan. We would to thank Barry Cooke for his guidance in field methods and SBW identification, and also the following people for assisting with the field data collection: Nate Aspelin, Louis-Etienne Robert, Brian Miranda, Robert Costanza, Barry Cooke, Stephane Bourassa, and Patrick James. The Superior National Forest provided housing during the field season and assisted with sampling logistics. – Remi St-Amant

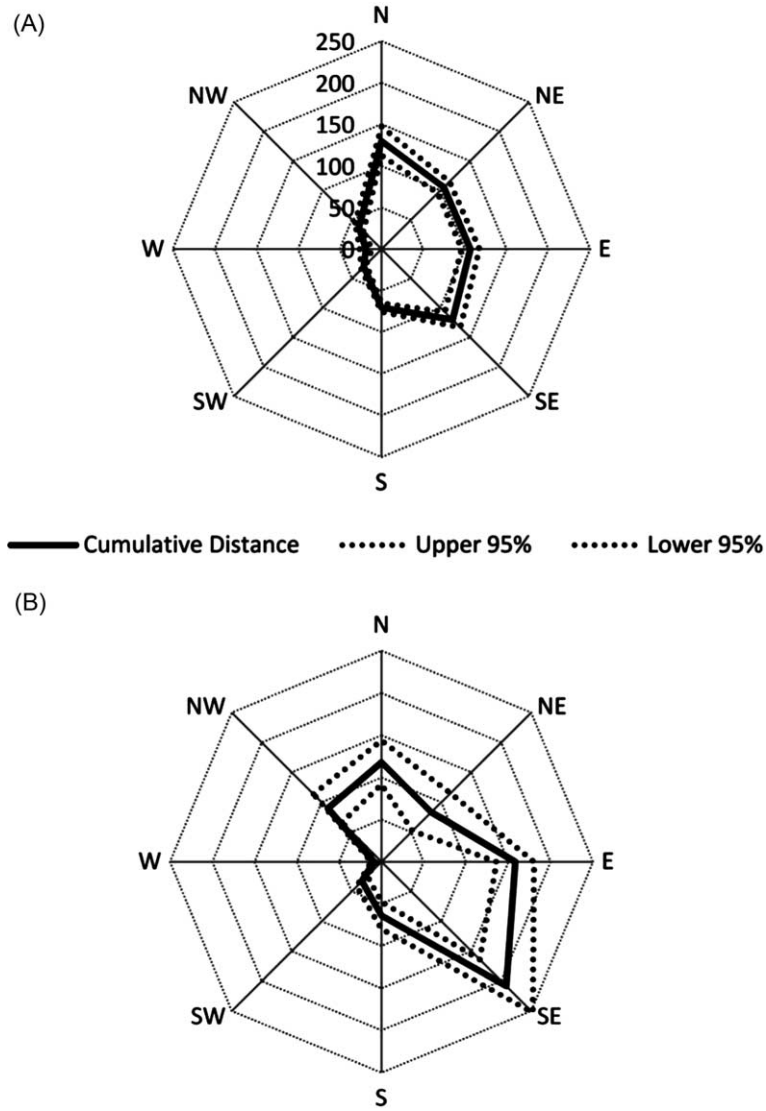

Figure 6. Independent wind analyses indicating prevailing wind patterns during periods of active moth flight for (A) all larvae collection points distributed across the study area, and (B) collection points with high relative larvae abundance (>0.75 larvae min^{-1} of search effort). Axis units are identical between graphs and represent distance (km) potentially travelled by a particle in a given direction when summed across the entire active male moth flight period.

assemble the necessary weather input data required to estimate the budworm adult flight window using BioSIM. Anouk Wanrooy assisted with the figures. We also thank Marie-Josée Fortin, Mandy Barron and 3 anonymous reviewers for helpful comments on the manuscript.

References

Batschelet, E. 1981. Circular statistics in biology. – Academic Press.

Bergeron, Y. et al. 1995. Balsam fir mortality following the last spruce budworm outbreak in northwestern Quebec. – Can. J. For. Res. 25: 1375–1384.

Blanchong, J. A. et al. 2002. Assignment of individuals to populations: Bayesian methods and multi-locus genotypes. – J. Wildl. Manage. 66: 321–329.

Candau, J. N. et al. 1998. Spatiotemporal patterns of large-scale defoliation caused by the spruce budworm in Ontario since 1941. – Can. J. For. Res. 28: 1733–1741.

Cappuccino, N. et al. 1998. Spruce budworm impact, abundance and parasitism rate in a patchy landscape. – Oecologia 114: 236–242.

Clark, J. S. 1998. Why trees migrate so fast: confronting theory with dispersal biology and the paleorecord. – Am. Nat. 152: 204–224.

Clark, J. S. 2007. Models for ecological data. – Princeton Univ. Press.

Clark, J. S. et al. 1999. Seed dispersal near and far: patterns across temperate and tropical forests. – Ecology 80: 1475–1494.

Cooke, B. J. and Roland, J. 2000. Spatial analysis of large-scale patterns of forest tent caterpillar outbreaks. – Ecoscience 7: 410–422.

Cooke, B. J. and Lorenzetti, F. 2006. The dynamics of forest tent caterpillar outbreaks in Québec, Canada. – For. Ecol. Manage. 226: 110–121.

Dale, V. H. et al. 2001. Climate change and forest disturbances. – Bioscience 51: 723–734.

ESRI 2006. ArcGIS: release 9.2 [software], 1999–2006. – Environmental Systems Research Inst.

Gage, S. H. et al. 1999. Ecological scaling of aerobiological dispersal processes. – Agric. For. Meteorol. 97: 249–261.
Gelman, A. and Rubin, D. B. 1992. Inference from iterative simulation using multiple sequences. – Stat. Sci. 7: 457–511.
Gelman, A. et al. 2004. Bayesian data analysis. – Chapman and Hall/CRC.
Greenbank, D. O. et al. 1980. Spruce budworm (Lepidoptera: Tortricidae) moth flight and dispersal: new understanding from canopy observations radar and aircraft. – Mem. Entomol. Soc. Can. 110: 1–49.
Hanski, I. et al. 1995. Multiple equilibria in metapopulation dynamics. – Nature 377: 618–621.
James, P. M. A. 2009. Interacting disturbances in the boreal forest and the importance of spatial legacies at multiple scales. – PhD thesis, Faculty of Forestry, Univ. of Toronto.
Johnson, D. M. et al. 2004. Landscape geometry and travelling waves in the larch budmoth. – Ecol. Lett. 7: 967–974.
Johnson, D. M. et al. 2006. Landscape mosaic induces traveling waves of insect outbreaks. – Oecologia 148: 51–60.
Kaitala, V. and Ranta, E. 1998. Travelling wave dynamics and self-organization in a spatio-temporally sturctured population. – Ecol. Lett. 1: 186–192.
Kareiva, P. 1990. Population dynamics in spatially complex environments: theory and data. – Phil. Trans. R. Soc. B 330: 233–270.
Keyghobadi, N. et al. 1999. Influence of landscape on the population genetic structure of the alpine butterfly *Parnassius smintheus* (Papilionidae). – Mol. Ecol. 8: 1481–1495.
Keyghobadi, N. et al. 2006. Fine-scale population genetic structure of a wildlife disease vector: the southern house mosquito on the island of Hawaii. – Mol. Ecol. 15: 3919–3930.
Lucchini, V. et al. 2002. Noninvasive molecular tracking of colonizing wolf (*Canis lupus*) packs in the western Italian Alps. – Mol. Ecol. 11: 857–868.
Manel, S. et al. 2002. Detecting wildlife poaching: identifying the origin of individuals with Bayesian assignment tests and multilocus genotypes. – Conserv. Biol. 16: 650–659.
Manel, S. et al. 2003. Landscape genetics: combining landscape ecology and population genetics. – Trends Ecol. Evol. 18: 189–197.
Martinez, I. and Gonzalez-Taboada, F. 2009. Seed dispersal patterns in a temperate forest during a mast event: performance of alternative dispersal kernels. – Oecologia 159: 389–400.
Mullen, M. A. et al. 1998. Influence of trap design and location on the capture of *Plodia interpunctella* (Indian meal moth) (Lepidoptera: Pyralidae) in a release–recapture study. – J. Stored Prod. Res. 34: 33–36.
Nathan, R. et al. 2005. Long-distance biological transport processes through the air: can nature's complexity be unfolded in silico? – Divers. Distrib. 11: 131–137.
Nealis, V. G. and Régnière, J. 2004a. Fecundity and recruitment of eggs during outbreaks of spruce budworm. – Can. Entomol. 136: 591–604.
Nealis, V. G. and Régnière, J. 2004b. Insect-host relationships influencing disturbance by the spruce budworm in a boreal mixedwood forest. – Can. J. For. Res. 34: 1870–1882.
Ockinger, E. and Smith, H. G. 2008. Do corridors promote dispersal in grassland butterflies and other insects? – Landscape Ecol. 23: 27–40.
Onstad, D. W. et al. 2003. Does landscape diversity slow the spread of rotation-resistant western corn rootworm (Coleoptera: Chrysomelidae)? – Environ. Entomol. 32: 992–1001.
Peltonen, M. et al. 2002. Spatial synchrony in forest insect outbreaks: roles of regional stochasticity and dispersal. – Ecology 83: 3120–3129.
Pritchard, J. K. et al. 2000. Inference of population structure using multilocus genotype data. – Genetics 155: 945–959.
Pulliam, H. R. 1988. Sources, sinks, and population regulation. – Am. Nat. 132: 652–661.
Régnière, J. 1982. A process-oriented model of spruce budworm phenology (Lepidoptera: Tortricidae). – Can. Entomol. 114: 811–825.
Régnière, J. and You, M. S. 1991. A simulation model of spruce budworm (Lepidoptera, Tortricidae) feeding on balsam fir and white spruce. – Ecol. Model. 54: 277–297.
Régnière, J. and Saint-Amant, R. 2004. BioSim 8.0. – Canadian Forest Service, Quebec.
Riley, J. R. et al. 1991. The long distance migration of *Nilaparvata lugens* (Stal) (Delphacidae) in China: radar observations of mass return flight in the autumn. – Ecol. Entomol. 16: 471–489.
Roland, J. 1993. Large-scale forest fragmentation increases the duration of tent caterpillar outbreak. – Oecologia 93: 25–30.
Royama, T. 1984. Population dynamics of the spruce budworm *Choristoneura fumiferana*. – Ecol. Monogr. 54: 429–462.
Royama, T. et al. 2005. Analysis of spruce budworm outbreak cycles in New Brunswick, Canada, since 1952. – Ecology 86: 1212–1224.
Rueness, E. K. et al. 2003. Ecological and genetic spatial structuring in the Canadian lynx. – Nature 425: 69–72.
Sanders, C. J. et al. 1978. Flight activity of female eastern spruce budworm (Lepidoptera: Tortricidae) at constant temperatures in the laboratory. – Can. Entomol. 107: 1289–1299.
Sharov, A. A. and Liebhold, A. M. 1998. Model of slowing the spread of gypsy moth (Lepidoptera: Lymantriidae) with a barrier zone. – Ecol. Appl. 8: 1170–1179.
Spiegelhalter, D. J. et al. 2002. Bayesian mesures of model complexity and fit (with discussion). – J. R. Stat. Soc. B 64: 583–639.
Stoyan, D. and Wagner, S. 2001. Estimating the fruit dispersion of anemochorous forest trees. – Ecol. Model. 145: 35–47.
Su, Q. et al. 1996. The influence of hardwood content on balsam fir defoliation by spruce budworm. – Can. J. For. Res. 26: 1620–1628.
Tobin, P. C. and Bjornstad, O. N. 2005. Roles of dispersal, stochasticity, and nonlinear dynamics in the spatial structuring of seasonal natural enemy-victim populations. – Popul. Ecol. 47: 221–227.
Wagner, S. et al. 2004. Directionality in fruit dispersal models for anemochorous forest trees. – Ecol. Model. 179: 487–498.
Walder, K. et al. 2009. Improving inverse model fitting in trees – anisotropy, multiplicative effects, and Bayes estimation. – Ecol. Model. 220: 1044–1053.
Westbrook, J. K. and Isard, S. A. 1999. Atmospheric scales of biotic dispersal. – Agric. For. Meteorol. 97: 263–274.
Wikle, C. 2003. Hierarchical Bayesian models for predicting the spread of ecological processes. – Ecology 84: 1382–1394.
Williams, D. W. and Liebhold, A. M. 2000. Spatial synchrony of spruce budworm outbreaks in eastern North America. – Ecology 81: 2753–2766.
Wisely, S. M. et al. 2004. Genetic diversity and structure of the fisher (*Martes pennanti*) in a peninsular and peripheral metapopulation. – J. Mammal. 85: 640–648.
Wolter, P. T. et al. 2009. Estimation of forest structural parameters using 5 and 10 meter SPOT-5 satellite data. – Remote Sens. Environ. 113: 2019–2036.
Zhang, Q. and Alfaro, R. I. 2003. Spatial syndrony of the two-year cycle budworm outbreaks in central British Columbia, Canada. – Oikos 102: 146–154.